Effect of bremsstrahlung radiation emission on distributions of runaway electrons in magnetized plasmas

O. Embréus,[1] A. Stahl,[1] S. Newton,[1,2] G. Papp,[3] E. Hirvijoki,[1] and T. Fülöp[1]
[1)] *Department of Applied Physics, Chalmers University of Technology, Gothenburg, Sweden*
[2)] *CCFE, Culham Science Centre, Abingdon, Oxon, OX14 3DB, United Kingdom*
[3)] *Max-Planck Institute for Plasma Physics, D-85748 Garching, Germany*

(Dated: 13 November 2015)

Bremsstrahlung radiation is an important energy loss mechanism for energetic electrons in plasmas. In this paper we investigate the effect of bremsstrahlung radiation reaction on the electron distribution in 2D momentum space. We show that the emission of bremsstrahlung radiation leads to non-monotonic features in the electron distribution function and describe how the simultaneous inclusion of synchrotron and bremsstrahlung radiation losses affects the dynamics of fast electrons. We give quantitative expressions for (1) the maximum electron energy attainable in the presence of bremsstrahlung losses and (2) when bremsstrahlung radiation losses are expected to have a stronger effect than synchrotron losses, and verify these expressions numerically. We find that, in typical tokamak scenarios, synchrotron radiation losses will dominate over bremsstrahlung losses, except in cases of very high density, such as during massive gas injection.

arXiv:1511.03917v1 [physics.plasm-ph] 12 Nov 2015

I. INTRODUCTION

Energetic electrons are ubiquitous in plasmas, and bremsstrahlung radiation is one of their most important energy loss mechanisms[1]. At sufficiently high energy, around a few hundred megaelectronvolts in hydrogen plasmas, the loss associated with the emission of bremsstrahlung radiation dominates the energy lost by the fast electron through elastic collisions. Bremsstrahlung can also strongly affect electrons at somewhat lower energies, around a few tens of megaelectronvolts, particularly in high-density plasmas where the magnetic field is not too strong.

An important electron acceleration process, producing energetic electrons in both space and laboratory plasmas, is the runaway mechanism[2]. This requires an electric field of intermediate strength, parallel to the magnetic field in a magnetized plasma: it must be stronger than a critical field to overcome the friction force that fast electrons experience due to collisions[3], while sufficiently weaker than the Dreicer field, above which the entire electron population will promptly be accelerated[2]. A fraction of the charged particles can then detach from the bulk population and accelerate to high energy, where radiative losses become important.

Disruptions in fusion devices can induce strong, time-dependent electric fields, leading to the generation of runaway electrons (REs) with energies reaching several tens of megaelectronvolts – it has been proposed that runaway electrons in ITER[4] would be able to reach energies on the order of 100 MeV[5]. These electrons could severely damage plasma facing components. A key issue for ITER and other future tokamaks is therefore to increase the understanding of the dynamics of these relativistic electrons, with the specific goal of reducing their energy and destructive potential[6]. Previous studies[7–11] have shown that the energy carried away by synchrotron and bremsstrahlung radiation can be important in limiting the energy of REs. This effect is especially pronounced during disruption mitigation when large amounts of high-atomic-number gas (e.g. neon or argon) is injected, leading to an increase in the effective charge of the plasma.

Kinetic modeling of electron runaway, accounting for the synchrotron radiation reaction, is required to obtain an accurate description of runaway electron distributions. Inclusion of the synchrotron radiation reaction has been found to both limit the growth rate of the RE population[12] and lead to the formation of non-monotonic features in the high energy tail of the distribution[10,11,13]. Similarly to synchrotron radiation, bremsstrahlung radiation is expected to change the fast electron distribution.

The reaction force on test particles has been extensively studied and it was pointed out that bremsstrahlung and synchrotron radiation are both effective in controlling the energy of runaway electrons[8,9,14]. A quantitative study of how bremsstrahlung affects the runaway electron distribution function, however, is yet to be carried out. In this work, we will recap the kinetic description of the bremsstrahlung process in optically thin plasmas. This serves to illustrate the physics involved, and also acts as a foundation for the derivation of a simplified model operator, valid for typical runaway scenarios and allowing a quantitative study of the effect of bremsstrahlung on runaway electron dynamics. This, together with a description of the linearized two-dimensional kinetic equation used in the study, is contained in Section II.

By extending the numerical tool CODE[15], we will in Section III study the effect of bremsstrahlung on the distribution of electrons in 2D momentum-space. From the distribution we will deduce the impact on the evolution of the fast-electron population, as well as how the synergy between bremsstrahlung and synchrotron affect the dynamics. We show that, because of the sensitive interaction between synchrotron force and pitch-angle scattering[10], a higher effective charge of the plasma does not tend to favor bremsstrahlung over synchrotron, unlike the results previously reported[8,9,14].

In particular we derive a simple rule-of-thumb for when

bremsstrahlung is more important than synchrotron for the evolution of the runaway population, and verify its validity numerically. The plasma parameters considered in this work primarily reflect those of electron runaway in tokamak plasmas, but the validity of the model and the conclusions (presented in Section V) are applicable to a broader range of plasma parameters.

II. BREMSSTRAHLUNG RADIATION REACTION

The kinetic theory of inelastic processes is well understood, and is described in detail in monographs on the subject such as Ref. 16. Yet, in this section we shall provide a brief but self-contained description of the kinetics of bremsstrahlung reactions, presented in a form that is suitable for the purposes of the present study.

Specifically, in this work, we consider fully ionized plasmas of arbitrary ion composition near equilibrium, but with a population of fast electrons present in the energy range $10 - 100\,\mathrm{MeV}$, such as those produced for example by runaway acceleration in tokamak plasmas. In this energy range, reactions are accurately described only by relativistic quantum theory. In this picture (in lowest-order perturbation theory), bremsstrahlung is a binary interaction between two charged particles, resulting in the emission of a photon.

The frequency of the bremsstrahlung radiation is assumed to far exceed the plasma frequency, so that collective radiation effects can be neglected, and the plasma is assumed to be optically thin. These conditions impose no significant restriction; as the photon energies are primarily of the same order as the incident electron energy, they correspond to frequencies of the order $f \sim 10^{15}\,\mathrm{Hz}$. The question of the optical depth will be briefly discussed in Sec. II A.

We start by describing the effect of binary interactions (also referred to as collisions) on the rate of change of the distribution function $f_a(t, \underline{\mathrm{x}}, \underline{\mathrm{p}})$ of some particle species a at time t, position $\underline{\mathrm{x}}$ and momentum $\underline{\mathrm{p}}$, defined such that $n_a(t, \underline{\mathrm{x}}) = \int \mathrm{d}\underline{\mathrm{p}}\, f_a(t, \underline{\mathrm{x}}, \underline{\mathrm{p}})$ is the number density of species a at $\underline{\mathrm{x}}$, and $N_a\{V\} = \int_V \mathrm{d}\underline{\mathrm{x}}\, n_a(t, \underline{\mathrm{x}})$ is the total number of particles a in a volume V at time t. From now on we suppress the time- and space dependence of all functions as the collisions will be assumed local in space-time, and we shall consider only spatially homogeneous plasmas.

A. Reaction rates

Bremsstrahlung reactions are inelastic Coulomb interactions in which a photon is emitted with 4-momentum $k = (k/c, \underline{\mathrm{k}})$, with $k = c|\underline{\mathrm{k}}|$ denoting the photon energy and $\underline{\mathrm{k}}$ the 3-momentum. The process can be fully described by a differential cross-section $\mathrm{d}\sigma_{ab} = \mathrm{d}\sigma_{ab}(\underline{\mathrm{p}}_1, \underline{\mathrm{p}}_2, \underline{\mathrm{k}}; \underline{\mathrm{p}}, \underline{\mathrm{p}}')$, determining the rate of interaction for collision events $(\underline{\mathrm{p}}, \underline{\mathrm{p}}') \mapsto (\underline{\mathrm{p}}_1, \underline{\mathrm{p}}_2, \underline{\mathrm{k}})$. Here $\underline{\mathrm{p}}$ and $\underline{\mathrm{p}}_1$ denote the momenta of particle a before and after the interaction, respectively, and similarly $\underline{\mathrm{p}}'$ and $\underline{\mathrm{p}}_2$ those of particle b. The case of elastic scattering corresponds to $\underline{\mathrm{k}} = 0$. The cross-section differential is over every degree of freedom of the process with the initial momenta $\underline{\mathrm{p}}$ and $\underline{\mathrm{p}}'$ given, constrained by conservation of momentum and energy. This can formally be expressed as

$$\begin{aligned}\mathrm{d}\sigma_{ab} = {} & \delta^3(\underline{\mathrm{p}} + \underline{\mathrm{p}}' - \underline{\mathrm{p}}_1 - \underline{\mathrm{p}}_2 - \underline{\mathrm{k}}) \\ & \times \delta(E + E' - E_1 - E_2 - k) A_{ab}\, \mathrm{d}\underline{\mathrm{p}}_1 \mathrm{d}\underline{\mathrm{p}}_2 \mathrm{d}\underline{\mathrm{k}}, \end{aligned} \tag{1}$$

where the (often complicated) function A_{ab} determines the numerical value of the cross-section. The above expression can be compared to Eq. (2.1) in Ref. 17, where further details on manipulations of the bremsstrahlung cross-section are provided. After removing the delta functions by appropriate integration over any four of the coordinates (one for each conservation law), the remaining cross-section is a differential in five variables. One additional coordinate can be eliminated due to the azimuthal symmetry of the unpolarized scattering process around the relative velocity of the incident particles in the center-of-mass frame.

The change $(\mathrm{d}n_a)_{c,ab}$ in the number density of species a due to collisions with particles of species b is given by[18,19]

$$\begin{aligned}\big(\mathrm{d}n_a\big)_{c,ab} = {} & f_a(\underline{\mathrm{p}}_1) f_b(\underline{\mathrm{p}}_2) \bar{g}_\varnothing \mathrm{d}\bar{\sigma}_{ab} \mathrm{d}\underline{\mathrm{p}}_1 \mathrm{d}\underline{\mathrm{p}}_2 \mathrm{d}t \\ & - f_a(\underline{\mathrm{p}}) f_b(\underline{\mathrm{p}}') g_\varnothing \mathrm{d}\sigma_{ab} \mathrm{d}\underline{\mathrm{p}} \mathrm{d}\underline{\mathrm{p}}' \mathrm{d}t. \end{aligned} \tag{2}$$

Here $g_\varnothing = \sqrt{(\underline{\mathrm{v}} - \underline{\mathrm{v}}')^2 - (\underline{\mathrm{v}} \times \underline{\mathrm{v}}')^2/c^2}$ is the Møller relative speed, being the relativistic generalization of the relative speed $v_\mathrm{rel} = |\underline{\mathrm{v}} - \underline{\mathrm{v}}'|$; it correctly reduces to v_rel in the non-relativistic limit and in the rest-frame of one particle its value is the speed of the other. In Eq. (2), a bar denotes a quantity for which we have let $\underline{\mathrm{p}}_1 \leftrightarrow \underline{\mathrm{p}}$ and $\underline{\mathrm{p}}_2 \leftrightarrow \underline{\mathrm{p}}'$, i.e. $\mathrm{d}\bar{\sigma}_{ab} = \mathrm{d}\sigma_{ab}(\underline{\mathrm{p}}, \underline{\mathrm{p}}', \underline{\mathrm{k}}; \underline{\mathrm{p}}_1, \underline{\mathrm{p}}_2)$, and similarly for $\bar{g}_\varnothing$.

The collision operator C_{ab} describing the rate of change of the distribution function at momentum $\underline{\mathrm{p}}$ due to collisions is formally introduced with the definition

$$C_{ab}(\underline{\mathrm{p}}) \equiv \left(\frac{\partial f_a}{\partial t}\right)_{c,ab} = \int \frac{(\mathrm{d}n_a)_{c,ab}}{\mathrm{d}t \mathrm{d}\underline{\mathrm{p}}}, \tag{3}$$

the integral to be taken over the variables indicated by Eq. (2) after factoring out the momentum volume element $\mathrm{d}\underline{\mathrm{p}}$. Equations (2) and (3) fully determine the rate of change of the distribution function at momentum $\underline{\mathrm{p}}$ due to collisions, and we can interpret the two terms in Eq. (2) as follows: The first term, the gain term, expresses the rate at which particles a are scattered *into* $\underline{\mathrm{p}}$ from $\underline{\mathrm{p}}_1$ due to all possible interactions with particles b of momentum $\underline{\mathrm{p}}_2$ in reactions $(\underline{\mathrm{p}}_1, \underline{\mathrm{p}}_2) \mapsto (\underline{\mathrm{p}}, \underline{\mathrm{p}}', \underline{\mathrm{k}})$. Likewise, the second term, the loss term, expresses the rate at which particles a are scattered *away* from $\underline{\mathrm{p}}$ due to all possible interactions with particles b of momentum $\underline{\mathrm{p}}'$, in interactions $(\underline{\mathrm{p}}, \underline{\mathrm{p}}') \mapsto (\underline{\mathrm{p}}_1, \underline{\mathrm{p}}_2, \underline{\mathrm{k}})$.

The differential cross-section can be split into separate contributions from elastic and inelastic scattering: $\mathrm{d}\sigma = \mathrm{d}\sigma^{(\mathrm{elastic})} + \mathrm{d}\sigma^{(\mathrm{inelastic})}$. Elastic scattering between particles is described by elastic Coulomb collisions, as the plasma has been assumed to be fully ionized. The inelastic interactions are dominated by bremsstrahlung reactions[1] which will be the focus of the remainder of this section, and the form of the bremsstrahlung cross-section will be given in Section II C. It will be illustrative to briefly investigate the form of Eqs. (2) and (3) for the elastic and inelastic cases separately, to highlight the challenges in kinetic modeling of inelastic collisions.

Elastic Coulomb collisions — For elastic processes ($\underline{\mathrm{k}} = 0$), Eq. (1) leaves only two variables when integrated over the delta functions, allowing a differential cross-section of the form $\mathrm{d}\sigma_{ab} = (\partial\sigma_{ab}/\partial\Omega)\mathrm{d}\Omega$, with Ω representing two scattering angles that parameterize any elastic collision with given incident momenta. We may here apply the *principle of detailed balance*, corresponding to the time-reversibility of mechanical systems[20] or quantum-mechanically to the symmetry of the transition matrix, valid for all processes in the spin-averaged Born approximation[1,21]. It expresses the symmetry of the reaction rates, and in the elastic case it takes the form[18]

$$\bar{g}_{\varnothing}\mathrm{d}\bar{\sigma}_{ab}\mathrm{d}\underline{\mathrm{p}}_1\mathrm{d}\underline{\mathrm{p}}_2 = g_{\varnothing}\mathrm{d}\sigma_{ab}\mathrm{d}\underline{\mathrm{p}}\mathrm{d}\underline{\mathrm{p}}'. \tag{4}$$

This allows Eq. (3) to be immediately written on the symmetric form normally referred to as the Boltzmann collision integral[22,23],

$$C_{ab}(\underline{\mathrm{p}}) = \int \mathrm{d}\underline{\mathrm{p}}'\mathrm{d}\Omega\, g_{\varnothing}\frac{\partial\sigma_{ab}}{\partial\Omega}\left[f_a(\underline{\mathrm{p}}_1)f_b(\underline{\mathrm{p}}_2) - f_a(\underline{\mathrm{p}})f_b(\underline{\mathrm{p}}')\right]. \tag{5}$$

As elastic Coulomb collisions are often dominated by grazing (small-angle, distant) collisions, the Boltzmann collision integral above can be reduced to an operator of the Fokker-Planck form[24]. The Fokker-Planck operator we use to account for elastic collisions in the plasma is described in Section II D.

Bremsstrahlung reactions — For bremsstrahlung, the situation is different, and a collision operator on the same symmetric form as for the elastic case can not be found. By combining Eqs. (2) and (3) one can always form the collision operator

$$C_{ab}(\underline{\mathrm{p}}) = \int \mathrm{d}\underline{\mathrm{p}}_1\, f_a(\underline{\mathrm{p}}_1)\int \mathrm{d}\underline{\mathrm{p}}_2\, \bar{g}_{\varnothing}f_b(\underline{\mathrm{p}}_2)\frac{\partial\bar{\sigma}}{\partial\underline{\mathrm{p}}} - f_a(\underline{\mathrm{p}})\int \mathrm{d}\underline{\mathrm{p}}'\, g_{\varnothing}f_b(\underline{\mathrm{p}}')\,\sigma, \tag{6}$$

where we introduced the two cross-sections $\partial\bar{\sigma}/\partial\underline{\mathrm{p}}$ and σ, obtained by integrating Eq. (1) over all remaining variables on the right-hand side. For elastic collisions, $\partial\bar{\sigma}/\partial\underline{\mathrm{p}}$ would retain one of the delta functions, while for inelastic processes the collision operator must be given on the above form.

C_{ab} is in general an integral operator containing six to eight integration variables, depending on how easily $\partial\bar{\sigma}/\partial\underline{\mathrm{p}}$ can be obtained. From a numerical point of view, evaluation of the bremsstrahlung cross-sections are often demanding due to large cancelations between terms in the limits of small emission angle or high or low photon energy. In addition, both $\partial\bar{\sigma}/\partial\underline{\mathrm{p}}$ and σ are generally logarithmically divergent expressions in the low-photon energy contributions (physically corresponding to a large number of low-energy photons being emitted, carrying a finite total energy). While the last issue can be resolved by cutting the integral off at photon wavelengths comparable to the dimension of the system, the evaluation of the cross-section is often computationally expensive.

Due to the infeasibility of integrating a detailed description of the bremsstrahlung process into current kinetic-equation solvers (because of its computational intensity), we will in the next section introduce a simplified model of the bremsstrahlung collision operator in Eq. (3), retaining some of its essential physical features while neglecting others. This will allow efficient solution of a kinetic equation suitable for runaway electrons, letting us quantify the importance of bremsstrahlung in magnetized plasmas where it, as an energy loss mechanism, competes primarily with synchrotron radiation.

Finally, to clarify the difference between the elastic and inelastic collision operators, the reason that the principle of detailed balance does not apply in the inelastic case is that it relates the bremsstrahlung cross-section to the reverse process where a photon is absorbed (inverse bremsstrahlung). However, as we assume the plasma to be optically thin, the emitted photons will promptly leave the plasma before interacting again with the energetic electrons. The validity of this assumption is readily verified: the multi-MeV bremsstrahlung photons (having frequencies $\omega \gg \omega_p$ much larger than the plasma frequency) primarily interact with the fast electrons through Compton scattering, for which the photon mean free path is of the order $\lambda \gtrsim 1/(n_{\mathrm{RE}}r_0^2) \approx (10^{29}\,\mathrm{m}^{-2})/n_{\mathrm{RE}}$, where $r_0 = e^2/(4\pi\varepsilon_0 m_e c^2)$ is the classical electron radius. As we are interested in runaway electron beams with typical densities $n_{RE} \ll 10^{20}$ m^{-3} and typically populating space with linear dimension of order L = 1-10 m, it is clear that emitted photons will not significantly interact again with the runaway electrons (the ratio of beam dimension and photon mean free path λ being $L/\lambda \ll 10^{-9}$). We may therefore neglect the presence of the photon distribution for the present study of runaway electron dynamics.

B. Single-particle model operator for bremsstrahlung

Due to the complexities of fully modeling bremsstrahlung interactions in the kinetic equation, we will seek a simpler form. *Ad-hoc*, we will assume a certain analytic form for the collision operator, and to uniquely specify its value we will demand that certain conditions – consistent with properties of the full collision operator in Eqs. (2) and (3) – are satisfied.

As we are interested in investigating the competition between accelerating electric field and bremsstrahlung as a slowing-down mechanism, it will be useful to look for a bremsstrahlung operator in the form of an effective single-particle force. Such a force would take the form of an operator

$$C^{(m)} = -\frac{\partial}{\partial \underline{\mathrm{p}}} \cdot \Big(\underline{\mathrm{F}}_{\mathrm{B}}(\underline{\mathrm{p}}) f_e(\underline{\mathrm{p}}) \Big), \tag{7}$$

where $\underline{\mathrm{F}}_B$ can be identified as the reaction force associated with the bremsstrahlung interactions. A condition that uniquely defines $\underline{\mathrm{F}}_B$ can be found by requiring that the model operator $C^{(m)}$ produces the same total radiated energy as the full collision operator for an arbitrary distribution function. The energy rate of change is defined as (using $\sqrt{m_e^2c^4 + p^2c^2} = \gamma m_e c^2$ for the particle energy)

$$\begin{aligned} W_{c,a} &\equiv \int \mathrm{d}\underline{\mathrm{p}}\, m_e c^2 \gamma \left(\frac{\partial f_a}{\partial t} \right)_c \\ &= m_e c^2 \sum_b \int \gamma \, (\mathrm{d}n_a)_{c,ab}/\mathrm{d}t. \end{aligned} \tag{8}$$

Due to the symmetry in performing the integration over all variables, we may let $(\underline{\mathrm{p}}_1, \underline{\mathrm{p}}_2) \leftrightarrow (\underline{\mathrm{p}}, \underline{\mathrm{p}}')$ in the first term of Eq. (2), yielding

$$W_{c,a} = -m_e c^2 \sum_b \int \mathrm{d}\underline{\mathrm{p}} \mathrm{d}\underline{\mathrm{p}}' \mathrm{d}\sigma \, g_\varnothing (\gamma - \gamma_1) f_a(\underline{\mathrm{p}}) f_b(\underline{\mathrm{p}}'). \tag{9}$$

The large mass difference between ions and electrons allows approximations to be made when calculating the energy radiated by the electron population, making it advantageous to treat the electron-ion and electron-electron interactions separately. In the electron-ion contribution, the characteristic speed of an ion in a population near equilibrium is much smaller than the electron velocities, $v_{Ti} = \sqrt{2T_i/m_i} \ll \sqrt{2T_e/m_e} = v_{Te}$, assuming T_e and T_i to be of the same order. Therefore, as the differential cross-section is a function of the center-of-mass energy and hence varies over scales of order the incident electron momentum, we may approximate the ion population as delta-distributed, $f_i(\underline{\mathrm{p}}') = n_i \delta(\underline{\mathrm{p}}')$. Conservation of energy allows us to relate $m_e c^2(\gamma - \gamma_1) = k$ when neglecting ion recoil effects, which are formally of order $\gamma m_e/m_i$. Consequently, we obtain a simpler relation for the energy loss rate:

$$W_{c,e\text{-}i} = -\sum_i n_i \int \mathrm{d}\underline{\mathrm{p}}\, v f_e(\underline{\mathrm{p}}) \int \mathrm{d}\sigma_{e\text{-}i}\, k. \tag{10}$$

For electron-electron interactions, the expression in Eq. (2) is symmetric with respect to permutations of $(\underline{\mathrm{p}}_1, \underline{\mathrm{p}}_2)$ and $(\underline{\mathrm{p}}, \underline{\mathrm{p}}')$ when integrated, as we now consider identical particles. Therefore, we may replace γ by $(\gamma + \gamma')/2$ and γ_1 by $(\gamma_1 + \gamma_2)/2$, yielding the energy rate

$$W_{c,e\text{-}e} = -\frac{1}{2} \int \mathrm{d}\underline{\mathrm{p}} \mathrm{d}\underline{\mathrm{p}}' \, g_\varnothing f_e(\underline{\mathrm{p}}) f_e(\underline{\mathrm{p}}') \int \mathrm{d}\sigma_{e\text{-}e}\, k, \tag{11}$$

where now $k = \gamma + \gamma' - \gamma_1 - \gamma_2$. This can be simplified to a form similar to the electron-ion case under the assumption that the fast-electron population can be treated as a perturbation to a sufficiently cold equilibrium. In that case, we may write $f_e = f_{e0} + f_{e1}$, where f_{e0} is the equilibrium solution and the perturbation f_{e1} includes the fast-electron population. In Eq. (11) we then find the term $f_e(\underline{\mathrm{p}}) f_e(\underline{\mathrm{p}}') = f_{e0}(\underline{\mathrm{p}}) f_{e0}(\underline{\mathrm{p}}') + f_{e0}(\underline{\mathrm{p}}) f_{e1}(\underline{\mathrm{p}}') + f_{e1}(\underline{\mathrm{p}}) f_{e0}(\underline{\mathrm{p}}') + f_{e1}(\underline{\mathrm{p}}) f_{e1}(\underline{\mathrm{p}})$. The last term, quadratic in the perturbation, can be neglected as f_{e1} is assumed small. In addition, the e-e bremsstrahlung cross-section vanishes in the limit where both incident electron velocities are much smaller than the speed of light, v, $v' \ll c$, as in that limit bremsstrahlung reduces to dipole radiation, with a two-electron system having zero dipole moment. Therefore, as long as the electron temperature satisfies $T_e \ll m_e c^2$, the first term, quadratic in the equilibrium distribution, is negligible[17]. The remaining two terms can be combined due to the symmetry between $\underline{\mathrm{p}}$ and $\underline{\mathrm{p}}'$ inside the integral, leaving the expression

$$W_{c,e\text{-}e} = -n_e \int \mathrm{d}\underline{\mathrm{p}}\, v f_e(\underline{\mathrm{p}}) \int \mathrm{d}\sigma_{e\text{-}e}\, k. \tag{12}$$

Here, it has further been assumed that $f_{e0}(\underline{\mathrm{p}}) = n_e \delta(\underline{\mathrm{p}})$, since the energies of the fast electrons far exceed the thermal energy.

An elementary calculation shows that the energy moment of the model operator given in Eq. (7) is

$$\begin{aligned} W^{(m)} &= \int \mathrm{d}\underline{\mathrm{p}}\, \gamma m_e c^2 C^{(m)} = \int \mathrm{d}\underline{\mathrm{p}}\, m_e c^2 \underline{\mathrm{F}}_{\mathrm{B}} \cdot \frac{\partial \gamma}{\partial \underline{\mathrm{p}}} f_e \\ &= \int \mathrm{d}\underline{\mathrm{p}}\, (\underline{\mathrm{v}} \cdot \underline{\mathrm{F}}_B) f_e, \end{aligned} \tag{13}$$

giving the same answer as $\sum_b W_{c,e\text{-}b}$ for any distribution function f_e, provided that we choose the bremsstrahlung reaction force as

$$\underline{\mathrm{F}}_B = -\hat{p} \sum_b n_b \int \mathrm{d}\sigma_{e\text{-}b}\, k. \tag{14}$$

While a component orthogonal to the momentum unit vector $\hat{p} = \underline{\mathrm{p}}/p$ would be consistent with the condition $W^{(m)} = W_{c,e}$, it can be ruled out on a physical basis since the force arises from the interaction with spherically symmetric background particle populations (delta-distributed in our linearized high-energy limit treatment), hence lacking any preferential direction except for that of the particle motion. By the same argument the force must also be independent of pitch-angle, and therefore represents isotropic friction.

A few remarks are in order regarding the approximation used above. The form in Eq. (14) for the

bremsstrahlung force is commonly employed as a simple model for electron slowing-down by bremsstrahlung[8,9,25], corresponding to the so-called radiation cross section often found in the literature[1,26].

While this form for the reaction force is both well-established and elementary, the derivation provided here illustrates the conditions for its validity, and also highlights the physics that is lost: in treating the bremsstrahlung collision process in the manner described above, two effects have been neglected. First, it is clear that the force operator in Eq. (7) describes only a continuous slowing-down of the electrons. Since the photons emitted in bremsstrahlung interactions often have energies of the same order as the incident electron, the slowing-down would in reality occur in leaps rather than continuously. In addition, as the photons are emitted in random directions and momentum is transferred to the target, the electrons are also deflected in the process (corresponding to a change in the pitch-angle), even though for an ensemble of electrons the angular deviation averages to zero. This would, akin to elastic Coulomb scattering, diffuse the electron distribution in momentum space, an effect which is not captured in the above treatment.

Finally, we remark that no energy is transfered from the electrons to the ions (which are assumed to be infinitely heavy), making Eq. (10) an accurate measure of the energy lost from the fast-electron population due to electron-ion bremsstrahlung radiation. However, in electron-electron interactions, energy will be transferred from the energetic electron not only to the photon, but also to the slow target particle. Therefore Eq. (11) is a lower bound for the energy loss of the fast-electron population. This can be compared to elastic scattering: since in that case $k \equiv 0$, the integral in Eq. (11) would vanish identically. However, electron slowing-down still occurs due to the energy transfer to the slow target electron, which would not be captured by this treatment.

Also note that, due to conservation of energy and since no energy is transfered to the ion species, $W_{c,e}$ denotes the total power emitted from the plasma as (bremsstrahlung) X-rays. By construction this is true also for $W^{(m)}$, limited only by the validity of the linearization procedure outlined above.

C. Cross-sections for bremsstrahlung emission

In this section we give explicit expressions for the bremsstrahlung reaction force. Due to the fundamental limitations of the model operator derived in the previous section, we will seek no greater accuracy in the cross-sections than that provided by the Born approximation in relativistic quantum theory. As we only consider fully ionized plasmas, we do not need to account for atomic form factors that would modify the formulas in the presence of bound electrons.

Electron-ion collisions — The cross-section for electron-ion bremsstrahlung interactions (with ions of charge Z) is given by the Bethe-Heitler formula[27]

$$\begin{aligned}\mathrm{d}^4\sigma = \frac{\alpha Z^2 r_0^2}{2\pi}\frac{p\sin\theta\sin\theta_0\mathrm{d}k\mathrm{d}\theta\mathrm{d}\theta_0\mathrm{d}\varphi}{p_0 k q^4}\\ \times\Bigg\{\frac{p^2\sin^2\theta}{(E-p\cos\theta)^2}(4E_0^2-q^2)\\ +\frac{p_0^2\sin^2\theta_0}{(E_0-p_0\cos\theta_0)^2}(4E^2-q^2)\\ -\frac{2pp_0\sin\theta\sin\theta_0\cos\varphi\,(4E_0E-q^2+2k^2)}{(E-p\cos\theta)(E_0-p_0\cos\theta_0)}\\ +2k^2\frac{p^2\sin^2\theta+p_0^2\sin^2\theta_0}{(E-p\cos\theta)(E_0-p_0\cos\theta_0)}\Bigg\},\end{aligned} \tag{15}$$

where $q = |\underline{\mathrm{p}}_0 - \underline{\mathrm{k}} - \underline{\mathrm{p}}|$ denotes the magnitude of the momentum transferred to the ion, $r_0 = e^2/(4\pi\varepsilon_0 m_e c^2) \approx 2.8\cdot 10^{-15}\,\mathrm{m}$ is the classical electron radius, $\alpha = r_0 m_e c/\hbar \approx 1/137$ is the fine-structure constant, e is the magnitude of the elementary charge, ε_0 is the vacuum permittivity, and all momenta and energies are normalized to $m_e c$ and $m_e c^2$, respectively. Subscript 0 denotes the incident electron, no subscript the outgoing electron, and k is the photon energy. We define θ_0 (θ) as the angle between incident (outgoing) electron and the emitted photon, while φ is the azimuthal angle (around the axis $\underline{\mathrm{k}}$) between incident and outgoing electron. The ion is assumed to be an infinitely massive scattering center, meaning that order $\gamma m_e/m_i$ recoil effects have been neglected.

This formula can be integrated analytically[28] to give the electron-ion bremsstrahlung reaction force (the sum over ion species is trivial since the ion parameters only appear in the charge factor Z_i^2 multiplying the cross-section),

$$\begin{aligned}F_{\mathrm{B},e\text{-}i}(p) &= -\sum_i n_i\int \mathrm{d}\sigma_{e\text{-}i}\,k\\ &= -\alpha Z_{\mathrm{eff}} n_e r_0^2 m_e c^2(\gamma-1)\\ &\times\left(\frac{4}{3}\frac{3\gamma^2+1}{\gamma p}\ln(\gamma+p) - \frac{(8\gamma+6p)}{3\gamma p^2}\Big(\ln(\gamma+p)\Big)^2\right.\\ &\left. -\frac{4}{3}+\frac{2}{\gamma p}\int_0^{2p(\gamma+p)}\mathrm{d}x\,\frac{\ln(1+x)}{x}\right),\end{aligned} \tag{16}$$

where $Z_{\mathrm{eff}} = \sum_i n_i Z_i^2/n_e$ is the effective charge of the plasma. In the high energy limit where $p^2 \approx \gamma^2 \gg 1$, this expression takes the asymptotic form

$$F_{\mathrm{B},e\text{-}i}(p) = -\frac{\alpha}{\pi}\frac{eE_c Z_{\mathrm{eff}}}{\ln\Lambda}(\gamma-1)\left(\ln 2\gamma - \frac{1}{3}\right), \tag{17}$$

where $E_c = n_e e^3\ln\Lambda/4\pi\varepsilon_0^2 m_e c^2 = 4\pi\ln\Lambda n_e r_0^2 m_e c^2/e$ is the critical electric field for runaway electron generation[3], defined as the minimum electric field above which runaway electrons can be generated in the absence of loss mechanisms other than collisional friction, and $\ln\Lambda$ is the Coulomb logarithm.

Electron-electron collisions — For e-e collisions, the full expression for the bremsstrahlung cross-section valid at all energies is unwieldy[29]. We will instead use the high-energy limit which, when integrated, yields a bremsstrahlung force of the same form as Eq. (17) but with $Z_{\rm eff} = 1$.

We then obtain for the full bremsstrahlung reaction, accounting for electron-ion and electron-electron interactions,

$$F_{\rm B}(p) = -\frac{\alpha(1+Z_{\rm eff})eE_c}{\pi \ln\Lambda}(\gamma-1)(\ln 2\gamma - 1/3). \quad (18)$$

This is the formula commonly used in the literature for the electron bremsstrahlung stopping power, for example given in Ref. 27, and used in Refs. 8, 9, and 14 to study electron slowing-down in plasmas. We can compare this expression for the force to a more accurate formula derived in Ref. 25, which was developed as a fit to numerical evaluations of the full bremsstrahlung cross-section in the Born approximation. These expressions are shown in Fig. 1 for the case $Z_{\rm eff} = 3$ and $\ln\Lambda = 15$, together with the friction force due to elastic Coulomb collisions.

It is seen that the agreement between our high-energy limit formula and the more accurate expression is excellent in the entire region where bremsstrahlung losses are significant compared to collisional friction. Due to the rapid fall-off of the bremsstrahlung force at low energy, the minimum friction is barely modified by the inclusion of bremsstrahlung losses, hence the critical electric field for runaway generation should largely be unaffected by its addition (certainly negligible within the order $1/\ln\Lambda$ accuracy of the Fokker-Planck equation).

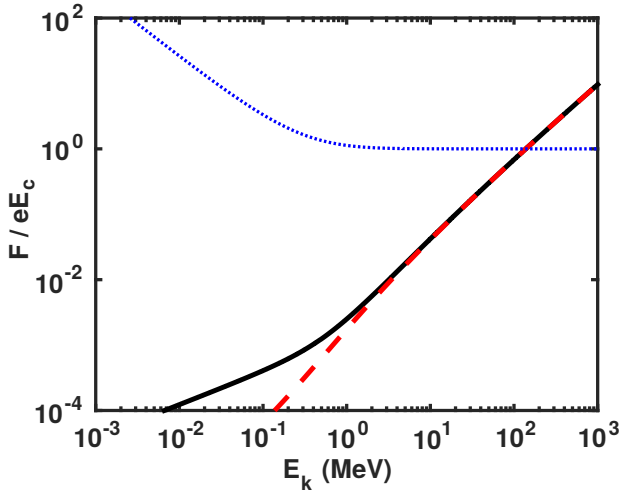


FIG. 1. Comparison of collisional energy losses in a plasma with constant $\ln\Lambda = 15$ and $Z_{\rm eff} = 3$. The lines represent numerical integration of the full Born-approximation bremsstrahlung radiation cross-section[25] (black, solid), the bremsstrahlung force used in this work (red, dashed), and the dynamical friction force associated with elastic Coulomb collisions (blue, dotted).

D. Kinetic equation and implementation in CODE

We wish to describe the time evolution of fast-electron populations under the influence of elastic and inelastic collisions, quasi-static electric fields and radiation reaction forces. We shall consider only plasmas where the Coulomb logarithm is large ($\ln\Lambda \gtrsim 10$) such that a Fokker-Planck treatment of the elastic Coulomb collisions is appropriate.

For the runaway problem we use a relativistic 0D+2V kinetic (Fokker-Planck) equation for the electron distribution,

$$\frac{\partial f_e}{\partial t} + \left\langle \frac{\partial}{\partial \underline{\rm p}} \cdot \left[(\underline{\rm F}_{\rm L} + \underline{\rm F}_{\rm S} + \underline{\rm F}_{\rm B}) f_e \right] \right\rangle = C_{ei} + C_{ee}. \quad (19)$$

Here $\underline{\rm p} = \gamma m_e \underline{\rm v}$ is the relativistic electron 3-momentum, $\underline{\rm F}_{\rm L}$ is the Lorentz force, while $\underline{\rm F}_{\rm S}$ and $\underline{\rm F}_{\rm B}$ denote the radiation reaction forces associated with synchrotron and bremsstrahlung radiation, respectively. The collision operators C_{ei} and C_{ee} describes the effect of elastic Coulomb collisions with ions and electrons. As we consider magnetized plasmas, the equation has been averaged over the gyro-motion (represented by the brackets), with

$$\left\langle \frac{\partial}{\partial \underline{\rm p}} \cdot (\underline{\rm F}_{\rm L} f_e) \right\rangle = -eE_\parallel \left(\frac{\partial}{\partial p} + \frac{1-\xi^2}{p}\frac{\partial}{\partial \xi} \right) f_e, \quad (20)$$

$$\left\langle \frac{\partial}{\partial \underline{\rm p}} \cdot (\underline{\rm F}_{\rm S} f_e) \right\rangle = -\frac{1}{\tau_{\rm S}} \left[\frac{1}{p^2}\frac{\partial}{\partial p}\left(\gamma p^3 [1-\xi^2] f_e\right) + \frac{1}{p}\frac{\partial}{\partial \xi}\left(\frac{p\xi}{\gamma}[1-\xi^2] f_e \right) \right], \quad (21)$$

$$\left\langle \frac{\partial}{\partial \underline{\rm p}} \cdot (\underline{\rm F}_{\rm B} f_e) \right\rangle = -\frac{m_e c}{\tau_{\rm B}} \frac{1}{p^2}\frac{\partial}{\partial p}\left[p^2(\gamma-1)(\ln 2\gamma - 1/3) f_e \right], \quad (22)$$

where $p = |\underline{\rm p}|$, $\underline{\rm E}$ is the electric field and the subscript $\parallel$ denotes the Cartesian component parallel to the magnetic field, $\xi = p_\parallel/p$ is the pitch-angle cosine, and the characteristic radiation reaction time scales $\tau_{\rm S}$ and $\tau_{\rm B}$ for synchrotron and bremsstrahlung respectively are

$$\tau_{\rm S} = \frac{6\pi\varepsilon_0 (m_e c)^3}{e^4 B^2}, \quad (23)$$

$$\tau_{\rm B} = \frac{\pi \ln\Lambda\, m_e c}{\alpha(1+Z_{\rm eff})eE_c} = \frac{\pi\ln\Lambda}{\alpha(1+Z_{\rm eff})}\tau_c, \quad (24)$$

where B is the magnetic field strength and $\tau_c = m_e c/(eE_c)$ is the characteristic time scale of elastic collisions for relativistic electrons of energy much greater than the thermal energy. A detailed derivation of this particular form of the kinetic equation can be found, e.g., in Ref. 10. Note that the same kinetic equation is valid also for cylindrically symmetric unmagnetized plasmas

$(B = 0)$, with $\|$ then denoting the direction of the electric field. Equation (19) has been implemented in the numerical initial-value Fokker-Planck solver CODE[15], which is used for all numerical results presented in this work.

As we are interested in the momentum space dynamics of the runaway electrons, only the test-particle part of the linearized electron-electron collision operator C_{ee} is retained. The ions are assumed to be stationary and infinitely massive, and C_{ei} therefore only describes pitch-angle scattering, while C_{ee} is an asymptotic matching of the non-relativistic test-particle operator and the high-energy limit of the relativistic test-particle operator, yielding good agreement with the exact operator across the full energy range.

In the following, we will use a parameter σ to characterize the relative strength of the synchrotron reaction force compared to collisions. It is defined as the ratio of the characteristic time-scales, and is given by

$$\sigma = \frac{\tau_c}{\tau_{\mathrm{S}}} = \frac{2\varepsilon_0}{3m_e}\frac{B^2}{n_e \ln\Lambda}. \tag{25}$$

III. GENERAL EFFECT OF RADIATION REACTION ON THE ELECTRON DISTRIBUTION FUNCTION

It was recently shown that the inclusion of the synchrotron radiation reaction force in the kinetic equation could induce the formation of non-monotonic features (a "bump") in the high energy tail of the electron distribution[10,11]. The formation of such bumps is a consequence of the interplay between an accelerating force (the electric field, $E > E_c$) and the presence of an effective friction which increases with particle energy and pitch-angle[11]. The presence of the bump effectively limits the maximum energy obtained by the runaways. Since our bremsstrahlung radiation reaction force is isotropic, it does not exhibit the same pitch-angle dependence as the synchrotron force. However, it will act to reduce the particle momentum, thereby also limiting the maximum attainable particle energy. Therefore, inclusion of bremsstrahlung radiation reaction is also expected to result in the formation of a bump.

Figure 2 shows examples of the electron distribution function, calculated using CODE, with synchrotron (S), bremsstrahlung (B), and both synchrotron and bremsstrahlung (S+B) radiation reaction effects included. Non-monotonic features are clearly formed in all three cases, but their characteristics are significantly different. In the case of synchrotron radiation only, the bump is not very pronounced and does not significantly restrict the runaway energy (for the parameters used), leading to a drawn-out tail. In contrast, the bremsstrahlung-only bump is a sharp feature, accompanied by strong gradients in p and significant spreading in pitch. The combined effect of synchrotron and bremsstrahlung radiation reaction leads to a bump that has a large extension in $p_{||}$, but which is clearly defined and efficiently limits the maximum particle energy. It thus exhibits features from both the pure-synchrotron and pure-bremsstrahlung bumps, but is accompanied by a strong reduction in the particle energy at the bump peak (what we will refer to as the *bump location*), compared to the other two cases.

The dynamics in the presence of both synchrotron and bremsstrahlung forces can be understood by the following argument: the synchrotron reaction force, proportional to $p_\perp^2$ at large energies, acts mainly to limit the perpendicular momentum of the fast electrons, while allowing them to accelerate in the parallel direction. However, once the electrons reach an energy for which $F_{\mathrm{B}} + |eE_\|| < 0$ the spherically symmetric bremsstrahlung reaction force will stop them from being further accelerated in the parallel direction. As the electron distribution builds up in this region of momentum space, the increasing perpendicular gradient will cause a diffusive perpendicular momentum flux of electrons due to pitch-angle scattering, making the synchrotron force increasingly significant. This suppresses further expansion in the perpendicular direction.

The distributions shown in Fig. 2 are no longer changing – the system has evolved long enough for the distribution in Figs. 2b and c to reach steady-state. In Fig. 2a, the distribution is in a quasi-steady state. In this case, the numerical grid is not large enough to contain the complete distribution, and as a consequence there is a constant outflow through the boundary of the simulation domain.

IV. RELATIVE IMPORTANCE OF BREMSSTRAHLUNG AND SYNCHROTRON RADIATION REACTION

A. Analytical estimate

As shown in the previous section, both synchrotron and brehmsstrahlung radiation reaction can have a strong effect on the distribution function. In many scenarios, however, one of them will be dominant. It is thus informative to find an approximate condition to determine the relative importance of these mechanisms. This may be accomplished by comparing the location of the local maximum produced in the runaway tail for the two radiation-reaction forces separately (while neglecting the effect of the other). For energies greater than this maximum, the distribution exhibits a rapid decay with energy; hence the location of the maximum can be regarded as an approximate upper limit for the electron energy (for the case of pure synchrotron losses, the parallel width of the bump can be significant as illustrated in Fig. 2, but the decay is asymptotically exponential with energy[10] and the probability of finding particles with energies much larger than the location of the maximum is low).

In Ref. 10, the particle momentum at the location of the maximum of the bump formed in the runaway tail due to the synchrotron reaction force was investigated.

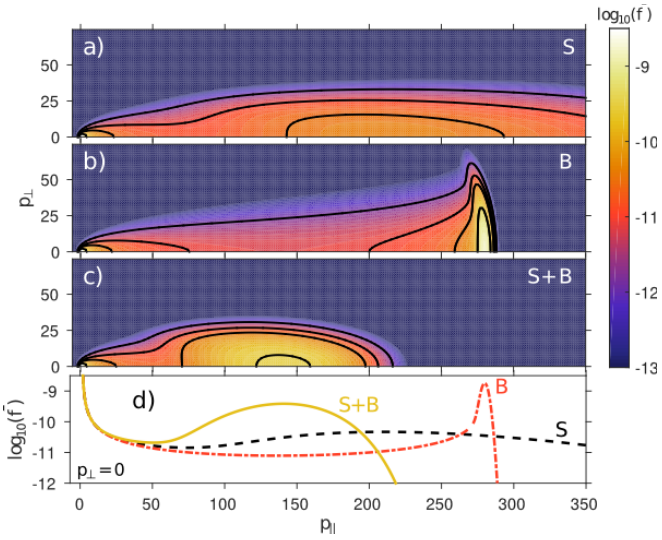


FIG. 2. Contour plots of electron distributions in 2D momentum space, exhibiting bumps induced by radiation reaction. Included reaction forces were a) synchrotron, b) bremsstrahlung and c) both synchrotron and bremsstrahlung. Cuts at $p_\perp = 0$ are shown in d). The distributions were obtained using CODE for the parameters $T_e = 10$ keV, $n_e = 2.3 \cdot 10^{21}$ m^{-3}, $B = 4$ T, $Z_{\rm eff} = 3$ and $E/E_c = 2$, after $t = 5 \cdot 10^5 \tau_{ee}$. The plotted quantity is $\log_{10}(\bar{f})$, where $\bar{f}$ is the distribution normalized so that $\bar{f}(p{=}0) = 1$.

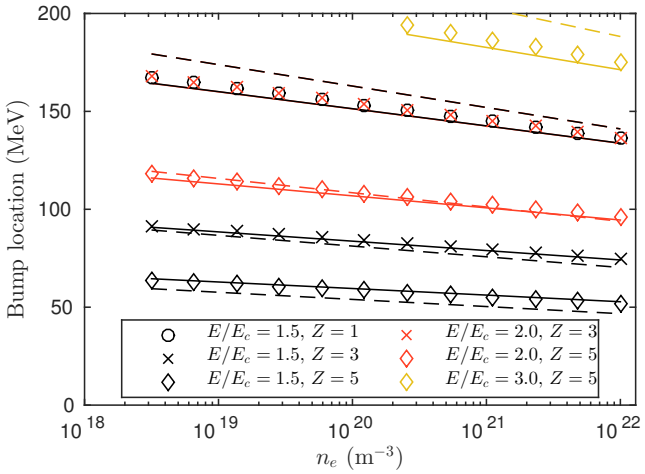


FIG. 3. Location of the bump in the distribution tail, induced by bremsstrahlung radiation reaction, for various combinations of density, electric field strength and effective charge. Symbols represent distributions obtained using CODE after $t = 5 \cdot 10^5 \tau_{ee}$, with $T_e = 10$ keV and neglecting synchrotron radiation reaction. The dashed and solid lines are the corresponding estimates for the bump location given by Eq. (28), using γ_0 corresponding to 100 MeV and taken from the location of the CODE bump, respectively. The agreement when using the more accurate value for γ_0 is excellent, but also the more rough value gives a good estimate for the actual bump location.

In the high energy limit, a lower bound in p,

$$p_{0\rm S} > \frac{1+\sigma}{\sigma}\frac{E/E_c - 1}{1+Z_{\rm eff}}, \tag{26}$$

was derived (where σ is given by Eq. 25). While the synchrotron force does not depend on $Z_{\rm eff}$ directly (since it is not a collisional effect), the synchrotron power radiated by an electron depends strongly on its pitch angle. The effective synchrotron force on a distribution of electrons is therefore directly proportional to the pitch-angle scattering term in the kinetic equation (as demonstrated in Ref. 10 and exhibited by Eq. 26), which does scale with the effective charge.

We can find a similar estimate for the maximum electron energy in the presence of bremsstrahlung (neglecting synchrotron effects) by considering force balance on a test particle. There are primarily three forces acting on an electron in the high energy limit: the accelerating force of the parallel electric field, collisional friction, and the bremsstrahlung reaction force. The maximum electron energy can be expected to approximately coincide with the momentum for which the forces balance, above which friction will be greater than the accelerating electric field. This yields the condition

$$eE - eE_c - \frac{1+Z_{\rm eff}}{\pi \ln\Lambda}\alpha e E_c \gamma(\ln 2\gamma - 1/3) = 0, \tag{27}$$

where we have used the high energy limit of both the bremsstrahlung reaction and collisional friction forces. We may find a simple expression by recognizing that in the last term, the logarithm varies slowly with energy and may be replaced by a characteristic value $\ln 2\gamma_0$, where γ_0 represents a typical energy scale for the local maximum of the runaway tail. Solving for $p_{0\rm B} \approx \gamma$ gives

$$p_{0\rm B} = \frac{\pi \ln\Lambda}{\alpha(\ln 2\gamma_0 - 1/3)}\frac{E/E_c - 1}{1+Z_{\rm eff}}. \tag{28}$$

This estimate for the location of the bump shows good agreement with distributions obtained using CODE, as demonstrated in Fig. 3.

It can be expected that bremsstrahlung will have a significant effect on the distribution (as compared to synchrotron radiation) when $p_{0B} \lesssim p_{0S}$, giving the condition

$$\frac{\pi \ln\Lambda}{\alpha(\ln 2\gamma_0 - 1/3)} \lesssim \frac{1+\sigma}{\sigma}. \tag{29}$$

The left-hand side is typically of order 10^3, thus corresponding to small values of σ. Therefore it is justified to neglect the term σ appearing in the numerator, and by inserting its definition from Eq. (25) we obtain a condition relating the magnetic field strength and electron density,

$$n_e \gtrsim \frac{2\pi}{3\alpha(\ln 2\gamma_0 - 1/3)}\frac{\varepsilon_0}{m_e}B^2. \tag{30}$$

With the electron density expressed in units of $10^{20}\,\mathrm{m}^{-3}$ and magnetic field expressed in Tesla, we find that bremsstrahlung effects become significant in limiting the maximum energy of runaway electrons for densities above

$$n_{e,\mathrm{lim}}[10^{20}\,\mathrm{m}^{-3}] \approx \frac{28}{\ln 2\gamma_0 - 1/3} B[T]^2. \tag{31}$$

For a typical location of the maximum electron energy at around $E_k = 100\,\mathrm{MeV}$, we obtain $n_{e,\mathrm{lim}}[10^{20}\,\mathrm{m}^{-3}] \simeq 5B[T]^2$. In Ref. 14 a similar condition was derived, showing a similar order of magnitude on the density $n_{e,\mathrm{lim}}$, but incorrectly suggesting that bremsstrahlung will be more important for larger Z_{eff}. The reason for this is that the test-particle picture employed in Ref. 14 does not accurately describe the pitch-angle scattering, hence the resulting synchrotron emission is underestimated.

In present day tokamak experiments, $n_e \lesssim 10^{20}\,\mathrm{m}^{-3}$ and $B \gtrsim 1\,\mathrm{T}$, indicating that the effect of bremsstrahlung radiation reaction is generally negligible. It will typically impose an energy limit an order of magnitude larger than that at which the synchrotron reaction force takes effect. Note, however, that Eq. (26) for the location of the distribution maximum caused by synchrotron radiation is a lower limit, accurate only to within a factor ~ 5 when compared to numerical results. This acts in favor of the importance of bremsstrahlung, so that a simple rule of thumb for the importance of bremsstrahlung effects (in place of Eq. 31) is

$$n_e[10^{20}\,\mathrm{m}^{-3}] \gtrsim B[T]^2. \tag{32}$$

It should be noted that in partially ionized plasmas containing high atomic number impurities, such as those produced during disruption mitigation scenarios with Massive Gas Injection in tokamaks, the bremsstrahlung will be enhanced compared to the expressions given here due to highly energetic electrons penetrating the charged cloud of electrons around the atomic nuclei. This effect is described by an atomic form factor which multiplies the cross-section formulas[30]. However, the same is true for elastic Coulomb collisions, as described in Ref. 31, leading to enhanced pitch-angle scattering with the consequence that the synchrotron force experiences a similar increase in efficacy. The enhanced scattering is thus not expected to significantly shift the balance between the bremsstrahlung and synchrotron forces. A full treatment of these effects, however, requires a detailed description of the atomic physics involved and is beyond the scope of this paper.

Curvature-induced synchrotron losses — It should be pointed out that, while the above is valid for straight field-line geometry, additional effects come into play in toroidal geometry. An additional energy loss through synchrotron radiation caused by the acceleration of the guiding center due to the toroidicity adds a frictional term similar to the bremsstrahlung radiation friction. In the high-energy limit, as derived in Ref. 7, this orbit-induced synchrotron radiation term takes the form

$$\left(\frac{\mathrm{d}p}{\mathrm{d}t}\right)_{\mathrm{orbit}} = -\frac{m_e c}{\tau_S}\frac{\rho_0^2}{R^2}\left(\frac{p_\parallel}{m_e c}\right)^4, \tag{33}$$

where $\rho_0 = m_e c/eB$ and R is the average radius of curvature of the magnetic field. To determine when this effect is important compared to the bremsstrahlung losses, we may investigate at what electron energy the two reaction forces become equal. Assuming that, for a runaway electron, it is valid to replace $p_\parallel \approx p \approx \gamma m_e c$, setting the loss terms as equal yields the condition

$$\frac{1}{\tau_B}\gamma \ln 2\gamma = \frac{1}{\tau_S}\frac{\rho_0^2}{R^2}\gamma^4, \tag{34}$$

where we have assumed $\gamma \gg 1$. Inserting numerical values for natural constants, we find

$$\frac{\gamma^3}{\ln 2\gamma} \approx (1 + Z_{\mathrm{eff}})1.2 \cdot 10^4 n_e[10^{20}\,\mathrm{m}^{-3}]R[\mathrm{m}]^2. \tag{35}$$

Assuming a characteristic $\ln 2\gamma = \ln 200 \approx 5.3$ – corresponding to runaway electron energies of approximately 50 MeV – we find that bremsstrahlung losses dominate orbit-induced synchrotron losses for relativistic factors smaller than

$$\gamma \approx 40\left((1 + Z_{\mathrm{eff}})n_e[10^{20}\,\mathrm{m}^{-3}]R[\mathrm{m}]^2\right)^{1/3}. \tag{36}$$

As we have previously indicated, bremsstrahlung radiation loss will be insignificant compared to the gyromotion-induced synchrotron radiation loss unless $n_e[10^{20}\,\mathrm{m}^{-3}] \gtrsim B[T]^2$. In tokamak plasmas this will primarily be the case during massive gas injection scenarios. Assuming a hypothetical ITER massive gas injection with $Z_{\mathrm{eff}} = 10$, $n_e = 10^{21}\,\mathrm{m}^{-3}$ and $R = 5\,\mathrm{m}$, we find that bremsstrahlung radiation loss will be dominant (as compared to the orbit synchrotron radiation loss) for all electrons with $\gamma \lesssim 560$, or energy lower than approximately 300 MeV. As a consequence, in typical scenarios of interest the orbit-induced synchrotron radiation loss will not affect our conclusions, although some care must be taken to ensure that expected runaway-electron energies are far from the threshold energy indicated by Eq. (36).

We may note that, unlike the synchrotron radiation caused by the gyromotion which is sensitive to pitch-angle scattering, the orbit-induced radiation loss tends to be less significant in comparison to bremsstrahlung radiation loss as the plasma effective charge increases. Its effect is also independent of magnetic field strength (cancelation occurring between τ_S and ρ_0), and thus only depends on particle energy and radius of curvature.

B. Numerical results

As discussed in Section III, bremsstrahlung effects can significantly reduce the average runaway energy under

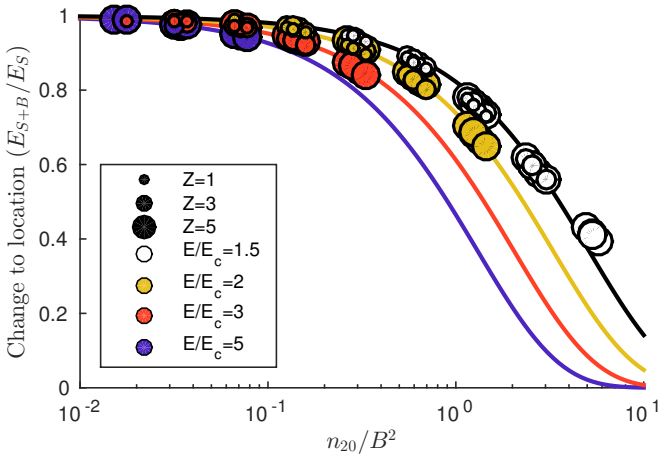


FIG. 4. Comparison between the location of the bump at $p_\perp = 0$ with and without bremsstrahlung radiation reaction effects included, as a function of the ratio of electron density and magnetic field squared. Circles denote CODE results, with Z_{eff} indicated by the size of the marker and E/E_c by the color. The solid lines are simple exponential fits to the data points, provided for visual guidance.

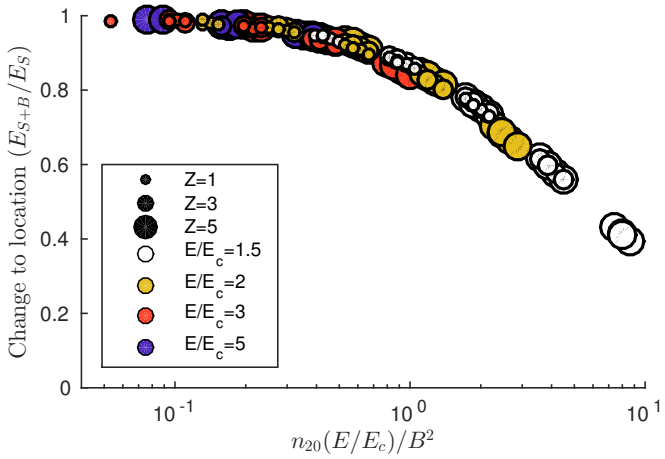


FIG. 5. The same as Fig. 4, except that the x-axis is weighted by an additional factor E/E_c.

those circumstances where it leads to a bump at lower particle energies than when considering only synchrotron radiation reaction. This shift in bump-on-tail location is one of the indicators of the importance of bremsstrahlung effects, and to quantify it we use CODE to study time-asymptotic electron distributions, for a variety of plasma parameters. Although the (quasi-)steady-state distribution function is not always of practical relevance in applications because of the time scales involved, this method allows us to quantify the relative importance of synchrotron and bremsstrahlung effects in a robust way.

Numerical distributions have been calculated for a variety of parameter sets, with parameters in the ranges: $n_e \in [3 \cdot 10^{18}, 1 \cdot 10^{22}]$ m^{-3}, $B \in [0, 4]$ T, $Z_{\text{eff}} \in [1, 5]$ and $E/E_c \in [1.5, 5]$, with and without bremsstrahlung radiation reaction included, for $T_e = 10$ keV. The results were analyzed after $5 \cdot 10^5$ thermal collision times, giving the distributions ample time to reach steady state.

Figure 4 shows a comparison of the location of the bump feature, with and without bremsstrahlung effects. Only data points where the entire bump was contained on the numerical grid in both the synchrotron-only and synchrotron-and-bremsstrahlung cases are included, and bumps located at energies below 9 MeV were omitted. The figure shows that the bump appears at lower energies as the density increases, with the change becoming significant for $n_e[10^{20}\,\text{m}^{-3}]/B[T]^2$ of order unity. This is in good agreement with the rule-of-thumb discussed in Section IV A. There is also no discernible dependence of the results on Z_{eff}, although the magnitude of the effect at a given n_e/B^2 increases with increasing E/E_c. While this dependence on the electric field is not explicitly described by the formulas derived in the previous section, it is not inconsistent with our treatment. This is because Eq. (26) describes only an approximate lower limit, correct within an order-unity coefficient that can depend on the other parameters. By numerically investigating the parametric dependence on the electric field strength, we find that a more accurate condition for the importance of bremsstrahlung effects is given by

$$\frac{E}{E_c} n_e[10^{20}\,\text{m}^{-3}] \gtrsim B[T]^2, \tag{37}$$

as illustrated in Fig. 5.

Another indicator of the relative importance of synchrotron and bremsstrahlung effects is the ratio of the power radiated by the two processes, as the process taking away the most energy is likely to have the largest impact on the distribution function. Figure 6 shows this ratio, in distributions obtained with both synchrotron and bremsstrahlung effects included. The emitted powers are calculated as the energy moments of the respective terms in the kinetic equation. We note that for $(E/E_c)n_e[10^{20}\,\text{m}^{-3}]/B[T]^2 \lesssim 4$, the radiated power is predominantly synchrotron radiation, whereas when $(E/E_c)n_e[10^{20}\,\text{m}^{-3}]/B[T]^2 \gtrsim 4$, bremsstrahlung is dominant. This reaffirms the conclusion drawn from Fig. 5 that bremsstrahlung starts to have a significant impact on the distribution at around $(E/E_c)n_e[10^{20}\,\text{m}^{-3}]/B[T]^2 \sim 1$. Again, there is no discernible dependence on Z_{eff}.

Looking directly at the distribution function can also provide important insight. Comparing the distributions in Fig. 7b (synchrotron and bremsstrahlung) to those in Fig. 7a (synchrotron only), it is clear that for the lowest densities shown, the distributions are very similar. The effect on the distribution is thus synchrotron-dominated in this case. For higher densities, the distributions do however become increasingly

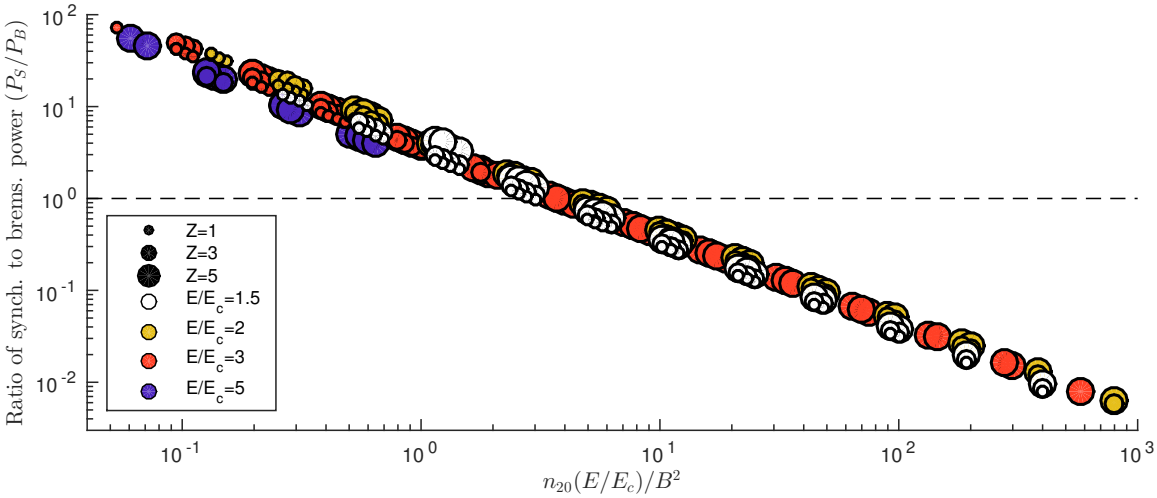


FIG. 6. Ratio of synchrotron to bremsstrahlung radiated power from distributions obtained with both synchrotron and bremsstrahlung effects included. Z_{eff} is indicated by the size of the marker and E/E_c by its color.

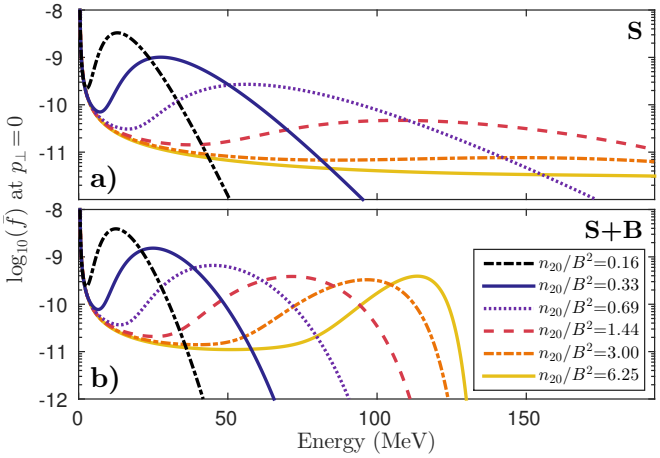


FIG. 7. Distributions at $p_\perp = 0$ for several values of n_e, with a) synchrotron and b) synchrotron and bremsstrahlung effects included. The parameters are $T_e = 10$ keV, $Z_{\text{eff}} = 3$, $E/E_c = 2$ and $B = 4$ T.

different, and above $n_e[10^{20}\,\text{m}^{-3}]/B[T]^2 \sim 1$ they are distinctly bremsstrahlung-dominated, as would be expected. Several different measures thus seem to agree that bremsstrahlung has an important effect on the fast electron distribution function for densities such that $n_e[10^{20}\,\text{m}^{-3}] \gtrsim B[T]^2$.

V. CONCLUSIONS

The effect of bremsstrahlung on the runaway electron distribution was investigated by extending the 2D Fokker-Planck equation solver CODE with a simplified description of the bremsstrahlung process, allowing rapid calculations. This method provides qualitative insight into the effect of bremsstrahlung on the distribution function, and allows for quantitative predictions of the maximum energy attainable by runaway electrons. In particular we have investigated the effect of bremsstrahlung radiation losses in combination with synchrotron radiation losses.

We show that the inclusion of bremsstrahlung losses leads to non-monotonic ("bump") features in the electron distribution function. Similar features have previously been described in the presence of synchrotron radiation, but bremsstrahlung leads to much stronger gradients in the magnitude of the momentum, as well as more significant spreading in pitch-angle. The combined effect of synchrotron and bremsstrahlung therefore leads to a bump that limits the particle energy more efficiently than in the case of pure synchrotron radiation reaction. From force balance considerations we derived an expression for the maximum electron energy, which shows excellent agreement with numerical simulations using CODE.

We show that if the condition $(E/E_c)n_e[10^{20}\,\text{m}^{-3}] \gtrsim B[T]^2$ is fulfilled, the effect of bremsstrahlung radiative losses on the electron distribution function are expected to be more important than synchrotron radiative losses. The importance of bremsstrahlung compared to synchrotron was found to be insensitive to plasma composition due to the similar parametric dependence on ion species of the bremsstrahlung reaction rate and pitch-angle scattering (related to the efficacy of synchrotron losses). This means that for typical tokamak-runaway scenarios we expect synchrotron radiation losses to dominate. In an ITER-like plasma with $B \simeq 5\,\text{T}$, for example, the required electron density for significant stopping power due to bremsstrahlung (as compared to synchrotron losses) is of order $n_e = 3\cdot 10^{21}\,\text{m}^{-3}$, which is significantly larger than the expected operational density of

order $n_e = 1 \cdot 10^{20}\,\mathrm{m}^{-3}$. However, in the case of massive gas injection for disruption mitigation, density increases of this order are possible, and in such scenarios it will be important to account for the bremsstrahlung losses, as well as synchrotron radiation losses, when modeling the slowing-down of fast electrons.

Note, finally, the limitations of the present study; we have considered steady-state solutions of the distribution function at low electric fields (E/E_c of order unity), where particle fluxes in momentum space are in balance. In transient processes, such as the initial slowing-down following a spike in the electric field strength, or other acceleration process, it is conceivable that the balance between bremsstrahlung and synchrotron losses is temporarily shifted before quasi-equilibrium is established. This typically happens on a time-scale of a few (relativistic) collision times $\tau_c = 4\pi\varepsilon_0^2 m_e^2 c^3/(e^4 n_e \ln\Lambda) \approx 0.3/(\ln\Lambda n_e[10^{20}\mathrm{m}^{-3}])\,\mathrm{s}$. Furthermore, as we have treated bremsstrahlung as a continuous process, the details of the shape of the distribution functions as shown in Figs. 2 and 7 should be considered only indicative. A more sophisticated treatment accounting for the finite photon energies is likely to lead to a broader bump on the runaway tail due to the diffusive nature of the resulting electron motion. However, we expect the qualitative trends (bump-on-tail formation, approximate location of the local maximum) to be well represented by the model adopted here. Finally, we have restricted this study to consider only fully ionized plasmas. In post-disruption plasmas with runaway mitigation by massive gas injection of high-Z atoms, where temperatures are often below 10 eV, both the bremsstrahlung and elastic scattering cross-sections are modified to account for the presence of bound electrons, due to incomplete screening of the charged nucleus at large incident energies. These effects would act to increase both the synchrotron (because of enhanced pitch-angle scattering) and bremsstrahlung losses compared to the predictions of our model, and a more detailed description of the atomic physics involved would be required for a more accurate simulation of such scenarios.

ACKNOWLEDGEMENTS

This work has been carried out within the framework of the EUROfusion Consortium and has received funding from the Euratom research and training programme 2014-2018 under grant agreement No 633053. The views and opinions expressed herein do not necessarily reflect those of the European Commission. This project has received funding from the Knut and Alice Wallenberg Foundation and Vetenskapsrådet.

[1] W. Heitler, The Quantum Theory of Radiation, Oxford University Press, London (1954).
[2] H. Dreicer, Phys. Rev. **115**, 2 (1959).
[3] J. W. Connor and R. J. Hastie, Nucl. Fusion **15**, 415 (1975).
[4] `http://www.iter.org`.
[5] G. Papp, M. Drevlak, T. Fülöp, P. Helander and G. I. Pokol, Plasma Phys. Control. Fusion 53, 095004 (2011).
[6] E. M. Hollmann, P. B. Aleynikov, T. Fülöp, D. A. Humphreys, V. A. Izzo, M. Lehnen, V. E. Lukash, G. Papp, B. Pautasso, F. Saint-Laurent and J. A. Snipes, Phys. Plasmas 22, 021802 (2015).
[7] F. Andersson, P. Helander, and L.-G. Eriksson, Phys. Plasmas **8**, 5221 (2001).
[8] M. Bakhtiari, G. J. Kramer, M. Takechi, H. Tamai, Y. Miura, Y. Kusama and Y. Kamada, Phys. Rev. Lett. 94, 215003 (2005).
[9] M. Bakhtiari, G. J. Kramer and D. G. Whyte, Phys. Plasmas 12, 102503 (2005).
[10] E. Hirvijoki, I. Pusztai, J. Decker, O. Embréus, A. Stahl and T. Fülöp, J. Plasma Phys. 81, 475810502 (2015).
[11] J. Decker, E. Hirvijoki, O. Embréus, Y. Peysson, A. Stahl, I. Pusztai and T. Fülöp, *Bump formation in the runaway electron tail*, `http://arxiv.org/abs/1503.03881`.
[12] A. Stahl, E. Hirvijoki, J. Decker, O. Embréus and T. Fülöp, Phys. Rev. Lett. 114, 115002 (2015).
[13] P. Aleynikov and B. N. Breizman, Phys. Rev. Lett. 114, 155001 (2015).
[14] I. Fernández-Gómez, J. R. Martín-Solís and R. Sánchez, Phys. Plasmas 14, 072503 (2007).
[15] M. Landreman, A. Stahl and T. Fülöp, Comp. Phys. Comm. **185**, 847 (2014).
[16] J. Oxenius, Kinetic Theory of Particles and Photons: Theoretical Foundations of Non-LTE Plasma Spectroscopy *in Springer Series in Electrophysics, Volume 20*, edited by Günter Ecker, Springer-Verlag, Berlin (1986).
[17] E. Haug, Z. Naturforsch. 30 a, 1546 (1975).
[18] C. Cercignani and G. M. Kremer, *The Relativistic Boltzmann Equation: Theory and Applications*, Springer Basel AG, Berlin (2002).
[19] H. Akama, J. Phys. Soc. Japan 28, 478 (1970).
[20] J. C. Light, J. Ross and K. E. Shuler, Rate Coefficients, Reaction Cross Sections and Microscopic Reversibility *in Kinetic Processes in Gases and Plasmas*, edited by A. Hochstim, Academic Press, New York (1969).
[21] S. Weinberg, *The Quantum Theory of Fields, Volume 1: Foundations*, Cambridge University Press, Cambridge (2005).
[22] E. M. Lifshitz, L. P. Pitaevskii, *Physical Kinetics*, Volume 10 in Course of Theoretical Physics, Elsevier Ltd, Oxford (1981).
[23] L. Boltzmann, *Vorlesungen über Gastheorie*, Verlag von Johann Ambrosius Barth, Leipzig (1896).
[24] L. Landau, Phys. Z. Sowjet. 10, 154 (1936).
[25] E. Haug, Astron. Astrohys. 423, 793 (2004).
[26] J. D. Jackson, *Classical Electrodynamics*, John Wiley & Sons, Inc., New York (1999).
[27] H. Bethe and W. Heitler, Proc. Roy. Soc. A 146, 83 (1934).
[28] G. Racah, Il Nuovo Cimento 11, 461 (1934).
[29] E. Haug and W. Nakel, *The Elementary Process of Bremsstrahlung*, World Scientific Publishing Co. Pte. Ltd., Singapore (2004).
[30] H. W. Koch and J. W. Motz, Rev. Mod. Phys. 31, 920 (1959).
[31] V. E. Zhogolev, S. V. Konovalov, VANT *or* Problems of Atomic Sci. and Tech. series Thermonuclear Fusion 37, 71 (2014) (in Russian) .